ULTRAFAST COMPTON SCATTERING X-RAY SOURCE DEVELOPMENT AT LLNL

F.V. Hartemann, A.M. Tremaine, S.G. Anderson, C. P. J. Barty, S. M. Betts, R. Booth, W. J. Brown, J.K. Crane, R.R. Cross, D.J. Gibson, D.N. Fittinghoff, J. Kuba, G. P. Le Sage, D.R. Slaughter, A.J. Wootton, E. P. Hartouni, and P.T. Springer, LLNL, Livermore, CA 94550, USA

J.B. Rosenzweig, UCLA, Los Angeles, CA 90095, USA

Abstract

Remarkable developments in critical technologies including terawatt-class lasers using chirped-pulse amplification, high-brightness photoinjectors, and high-gradient accelerators make it possible to design and operate compact, tunable, subpicosecond Compton scattering x-ray sources for a wide variety of applications. In such novel radiation sources, the collision between a femtosecond laser pulse and a low emittance relativistic electron bunch in a small (μm^3) interaction volume produces Doppler-upshifted scattered photons with unique characteristics: the energy is tunable in the 10-200 keV range, the angular divergence of the beam is small (mrad), and the pulses are ultrashort (10 fs – 10 ps). Currently, the PLEIADES facility produces > 2 x 10^7 photons per pulse in the 40-140 keV range, at 10 Hz, and has produced radiographs of high-Z materials, such as Ta and U; the γ^2-tunability of the source has also been demonstrated. These experimental results are discussed in detail and compared to theory. Future plans to improve the x-ray performance are also presented, as well as a new design for ultrafast, high contrast Bragg diffraction experiments on high-Z metal crystals.

INTRODUCTION

In recent years there has been, and there continues to be considerable interest in developing compact, ultrafast, bright x-ray sources for *in situ* dynamic material probing, flash radiography, and other important applications. Such novel sources include laser-driven K_α radiation systems, laser-driven plasmas, and high harmonic generators; considerably larger devices include free-electron lasers and synchrotrons, where slicing techniques can produce sub-picosecond x-ray pulses, albeit with a significant decrease in brightness and dose.

In view of the above, LLNL has created a development program based on Compton scattering, whereby an ultrahigh intensity laser pulse collides with a high-brightness, relativistic electron beam to produce tunable hard x-rays within a compact system. The radiation frequency on-axis is given by the Doppler upshift: $\omega_x = 4\gamma^2\omega_0$, where γ is the electron beam relativistic factor, while $\hbar\omega_0/e = 1.55$ eV at 800 nm. This approach has been enabled by remarkable developments in critical technologies including terawatt-class lasers using chirped-pulse amplification (CPA), high-brightness photoinjectors, and high-gradient accelerators.

Therefore, the main goal of this program was to design, model, assemble, commission and characterize a prototype to demonstrate that the aforementioned technologies can be integrated to produce high-brightness x-rays that can be tuned in the 30 – 100 keV range, and to benchmark a suite of three-dimensional codes predicting the x-ray characteristics given the full laser and electron beam phase spaces.

A further goal of this program is to demonstrate a series of applications including high-contrast radiography in high-Z metals, and dynamic diffraction using pump-probe techniques.

In this paper, the main subsystems of the PLEIADES (Picosecond Laser-Electron Inter-Action for the Dynamic Evaluation of Structures) Compton scattering x-ray source are described; the x-rays produced are then characterized and compared to theory.

EXPERIMENTAL SETUP

PLEIADES comprises five main subsystems: a 10 TW, 10 Hz CPA laser called FALCON; a high-brightness S-band rf photoinjector, which is driven by a UV laser; a 150 MeV S-band linac; finally, the Compton scattering interaction region and x-ray, electron beam, and laser diagnostics.

FALCON Laser

The main laser system used for these experiments is a Ti:Al_2O_3 CPA system capable of producing over 1 J of uncompressed light near 820 nm. The laser system front-end is a Ti:Al_2O_3 oscillator, which produces 30 fs pulses with a bandwidth of 36 nm centered at 815 nm. This mirror-dispersion-controlled Kerr-lens mode-locked laser also serves as the master clock for the entire experimental facility, ensuring synchronization between the laser and electron systems.

The oscillator pulses are stretched to 680 ps in an all-reflective parabolic-mirror based expander. The pulse train is then split with a dielectric beam splitter into two beams, with 30% of the light being coupled into a fiber to seed the photoinjector laser, and the remaining 70% used to seed the FALCON laser. Because the same oscillator pulse train seeds both laser systems, minimal timing jitter between the systems is assured.

In the FALCON laser, the oscillator pulses are amplified to an energy of 7.3 mJ in a standard linear regenerative amplifier cavity, pumped with 45 mJ of 532 nm light. Following the regenerative amplifier is a 4-pass

amplifier, which is pumped with the remaining 212 mJ of light from the pump. The output energy of this amplifier is 68 mJ. This beam is then sent into a second 4-pass amplifier, which also has a closed-loop feedback system to maintain input alignment. This amplifier is pumped by 2.3 J of 532-nm, and produces 1.2 J of uncompressed IR light.

The amplified light beam is expanded and collimated to a 1/e2 radius of 42 mm; the beam is then relay-imaged over 52 m, using two telescopes, to a vacuum chamber near the accelerator system, where it is compressed in a double-pass grating-compressor. A frequency-resolved, optically-gated GRENOUILLE system is used to measure the compressed pulses at low power, and yields a pulse length of 54 fs IFWHM, with a relative phase retrieval error of 0.006. The compressed pulse then propagates 20 m to the final focusing optics, currently an f:25 off-axis parabola. The loss through the transport and compressor is 45%, leaving up to 540 mJ available in the interaction region.

Photoinjector and Linac

The high-brightness electron beam used to generate x-rays at PLEIADES is produced by the LLNL 100-MeV linear electron accelerator, which has been substantially upgraded to meet the stringent emittance and timing jitter requirements necessary for efficient Compton scattering. The most significant upgrade was the installation of a new photoinjector at the front-end of the accelerator, as an alternative to the preexisting thermionic injector. In the S-band photoinjector, a high charge (nC), picosecond electron bunch is produced via the photoelectric effect when a UV laser pulse illuminates the photocathode. The photoemission threshold for the Cu photocathode is 266 nm, but this value is significantly relaxed by the strong Schottky effect induced by the 80–100 MeV/m rf field applied to the photocathode; indeed, the central wavelength of the UV beam produced after frequency-tripling is only 269 nm, but sufficient to obtain a quantum efficiency near 10^{-5}.

The rf photoinjector used to produce the electron beam for PLEIADES is based on a 1.6-cell standing-wave geometry. A pulsed S-band (2.8545 GHz) rf input with 7-MW peak power and 3-μs duration produces a peak axial electric field of up to 100 MV/m that accelerates the electrons to 5 MeV. Focusing solenoids are employed in the photoinjector to preserve the transverse emittance of the electron bunch, help match the electron beam into the accelerating sections, and to implement emittance compensation.

The beam generated by the photoinjector is then coupled into the 100 MeV linear electron accelerator, where it is accelerated to energies ranging between 20 and 100 MeV by four 1.8 meter, SLAC-type traveling-wave accelerating sections.

After propagating through the interaction area, the electron beam is deflected by a 30°-bend dipole magnet that separates the bunch from the scattered x-rays, which propagate in the same direction as the electrons. This dipole also serves as a spectrometer, yielding detailed measurements of the electron beam energy and energy spread, which is as low as 0.2%. Following the energy spectrometer, the electron beam is stopped in a Cu collector that also serves as a calibrated Faraday cup, providing a measure of the electron bunch charge. The electron collector is housed in a 10 cm-thick lead enclosure to minimize the effect of bremsstrahlung on the diagnostics.

X-Ray Interaction Region

The layout of the PLEIADES interaction region is shown in Fig. 1. The 540 mJ IR laser pulse is focused off a 60" focal length, 12° off-axis parabolic mirror. The focusing beam is then directed to the interaction region by a motor-controlled dielectric mirror, which allows for control of the transverse alignment of the laser focus at the interaction point. The spot is observed to have an average $1/e^2$ radius of 32 mm; the average M^2 is 1.4. In this case, the Rayleigh range, which defines the interaction region in the 180° geometry, is 2.86 mm.

The electron beam is focused by a set of quadrupole magnets with a magnetic field gradient of up to 15 T/m. To aid alignment at the focus, two cross-oriented dipole magnets steer the beam into this composite magnetic lens. Because the off-axis parabolic mirror that focuses the laser is fixed, the longitudinal position of the interaction region is set by the laser focus, and the longitudinal position of the electron beam waist is adjusted to the position of the laser focus using the electron focusing system. Measurements of the electron beam at the focus have shown a spot size of 27 μm, a normalized horizontal emittance of 3.5 mm.mrad, and a normalized vertical emittance of 11 mm.mrad, which were measured using the quadrupole scan technique.

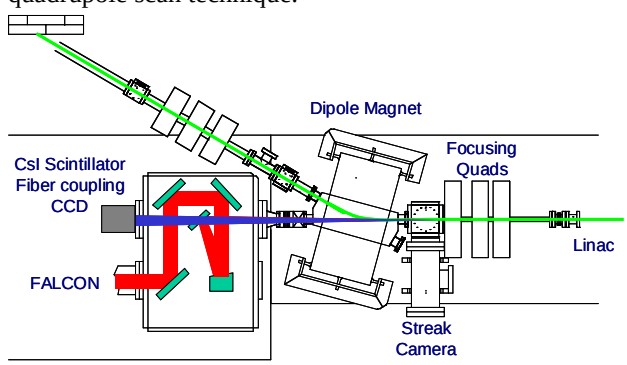

Fig. 1 X-ray interaction region.

EXPERIMENTAL RESULTS

In this section, a number of important x-ray measurements are highlighted and compared with theory, including the x-ray dose and energy-integrated angular distribution, x-ray dose as a function of delay between the laser and electron beams, determination of the x-ray spectrum scattered on-axis, and K-edge radiography in Ta and U.

In Fig. 2, the x-ray angular energy distribution is shown for experiments (left) and theory (right); the agreement is

excellent and the corresponding x-ray dose is 2 x 10^7 photons/shot. The theory is fully three-dimensional and accounts for the electron beam emittance, x-ray transmission through the BK7 folding mirror (see Fig. 1), and numerous other details.

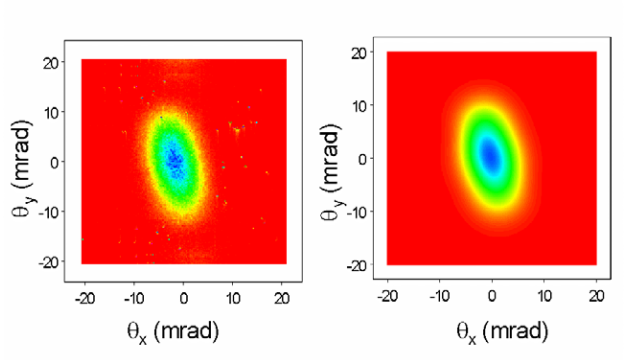

Fig. 2 X-ray angular energy distribution.

In Fig. 3 the peak on-axis x-ray brightness is reconstructed from a set of transmission measurements through Al foils, as shown in blue, and compared to computer simulations; the corresponding peak brightness is approximately 10^{17} photons/(mm^2 x mrad^2 x s x 0.1% bandwidth).

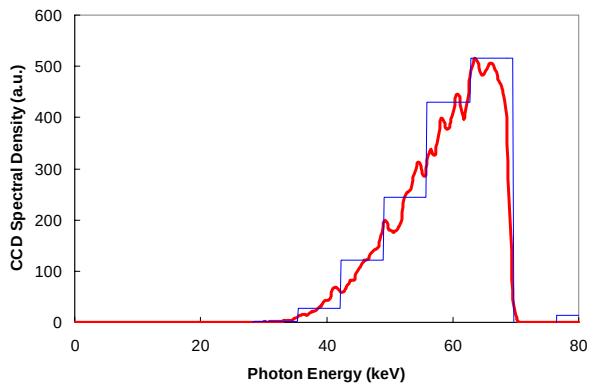

Fig. 3 On-axis spectral brightness.

The timing between the laser pulse and the electron bunch can be varied by using an optical delay line, and allows for measuring the scattered x-ray dose as a function of the synchronization between the two beams. Theoretically, the dominant effect for the 180^o interaction geometry and the PLEIADES parameters, where the inverse beta-function of the electron beam optics is much longer than the diffraction length of the laser, and where the electron bunch duration is much longer than the laser pulse, is the Rayleigh range determined by the laser focusing optics and beam quality. For the specific measurements presented in Fig. 4, M^2 = 1.45, w_0 = 37 μm, and the central laser wavelength is 815 nm; the dose is expected to vary as a Lorentzian with a HWHM equal to 12.1 ps, which is superimposed to the experimental data on Fig. 4; the agreement is quite good. The asymmetry probably results from the fact that the electron bunch carries more charge near its front end.

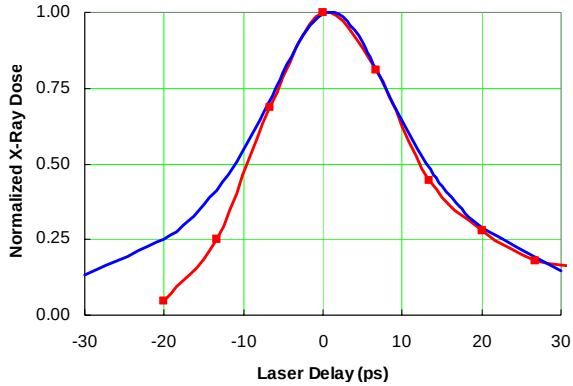

Fig. 4 Dose vs. delay.

Finally, Figure 5 demonstrates the γ^2-tuning of Compton scattering as well as the correlation between the scattering angle and the x-ray photon energy. The electron beam is first tuned so that the radiation energy on-axis lies just above the K-edge of Ta; as a result the on-axis photons are strongly absorbed as shown on the left of the figure. Off-axis photons have a lower energy, and are transmitted below the edge. By tuning the beam energy from 55 to 57 MeV, the photon energy on-axis is increased sufficiently to obtain significant transmission; off-axis photons with energies lying just above the edge are strongly absorbed, forming a dark ring structure. The agreement between theory (bottom) and experiment (top) is quite good.

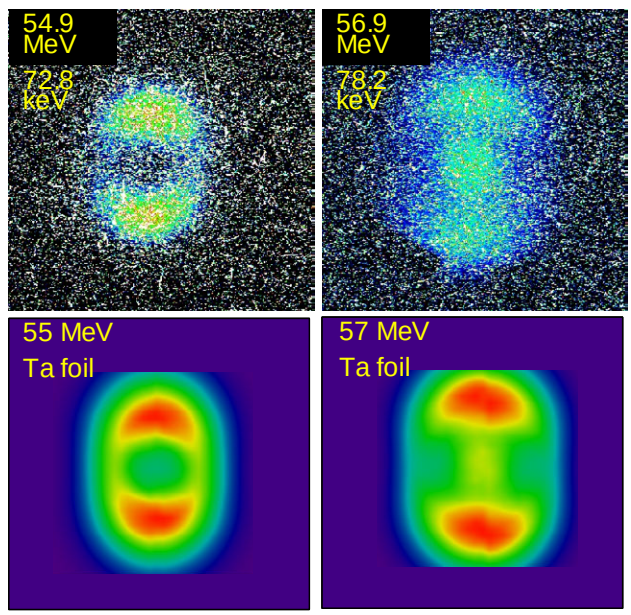

Fig. 5 Radiographs of Ta K-edge.

ACKNOWLEDGEMENTS

This work was performed under the auspices of the U.S. Department of Energy by University of California, Lawrence Livermore National Laboratory under Contract W-7405-Eng-48.